Molecular view of the isothermal transformation of a stable glass to a liquid

Stephen F. Swallen,[1] Kenneth L. Kearns,[1] Sushil Satija,[2] Katherine Traynor,[1] Robert J. McMahon,[1] and M. D. Ediger[1,a)]
[1]*Department of Chemistry, University of Wisconsin–Madison, Madison, Wisconsin 53706, USA*
[2]*NIST Center for Neutron Research, National Institute of Standards and Technology, Gaithersburg, Maryland 20899, USA*

(Received 21 December 2007; accepted 11 April 2008; published online 6 June 2008)

We have used neutron reflectivity to measure translational motion on the nanometer length scale in exceptionally stable glasses of tris(naphthylbenzene). These glasses are prepared by vapor deposition onto a substrate held somewhat below the glass transition temperature (T_g=342 K). When the most stable samples are annealed at 345 K, no translational motion is observed on the 12 nm length scale for over 10 000 s and full mixing requires more than 60 000 s. For comparison, the equilibrium supercooled liquid mixes in 1000 s at this temperature and on this length scale. These measurements provide insight into the mechanism by which a stable glass transforms into a liquid. "Melting" of the stable glass appears to occur by the growth of liquid regions into the surrounding glassy matrix, perhaps by a surface-initiated growth process. At 345 K, translational motion in the stable glass is at least 100 times slower than motion in the supercooled liquid. © *2008 American Institute of Physics*. [DOI: 10.1063/1.2919570]

INTRODUCTION

While a typical organic molecule has one liquid state and perhaps a few different crystal states, it can form a vast number of distinct glasses. Glasses are typically prepared by cooling a liquid. During cooling, the system undergoes kinetic arrest when the structural relaxation time of the liquid exceeds the time available for equilibration. Below this temperature, which is known as the glass transition temperature T_g, the molecules cannot reach configuration characteristics of the (metastable) equilibrium supercooled liquid. Glasses prepared at different cooling rates have different enthalpies, densities, and structures.

Glasses with low enthalpies and high densities are particularly interesting materials. In many senses, they are more stable than other glasses. For example, such glasses are less susceptible to environmental perturbations such as water uptake,[1] and they exhibit greater dimensional stability.[2] When heated, the molecules remain trapped in a particular glassy structure longer than for less stable glasses.[3] Unfortunately, it is not easy to prepare glasses with low enthalpies and high densities by cooling a liquid or aging a glass. Molecular rearrangements in a glass are extremely slow and these rearrangements are required for a less stable glass to spontaneously transform into a more stable glass. Kovacs has performed perhaps the best-known aging measurements, studying volume changes in polyvinylacetate glasses.[4] He was able to prepare highly relaxed glasses after 2 months of isothermal annealing at 298 K ($\sim T_g$-10 K). These materials were 0.5% more dense than the glass that formed immediately after cooling the polymer liquid at a few K/min.

Recently, we have shown that extremely stable glasses can be prepared by vapor deposition.[3,5,6] By holding the substrate temperature $T_{substrate}$ somewhat below T_g, we have made glasses with very low enthalpies, high kinetic stabilities, and high densities. For example, a thin glassy film of tris(naphthylbenzene) (TNB) was prepared with a density 1.7% larger than the conventional glass prepared by cooling the supercooled liquid.[3] The characteristics of these vapor-deposited glasses sensitively depend on the substrate temperature, with maximally stable films produced at $T_{substrate} \approx 0.85T_g$. We have shown that these stable glasses form because dynamics at the glass surface are many orders of magnitude faster than dynamics in the bulk.[3,5,6] This mobility means that molecules within a few nanometers of the surface have enough time to find efficient ways of packing before they are buried by further deposition. Studies of other small molecule organic glass formers have recently indicated that maximum stability is achieved at a substrate temperature near $0.85T_g$, indicating that this is a critical parameter in the preparation of stable glasses by physical vapor deposition.[5,7]

Here, we investigate the properties of vapor-deposited TNB glasses by using neutron reflectivity (NR). Alternating layers of protio- and deuterio-TNB are vapor deposited to produce a diffraction grating for neutrons. Multiple diffraction peaks are measured, extending up to the 17th harmonic in some cases. As the protio and deuterio layers intermix, the diffraction intensity is attenuated, allowing a quantitative assessment of translational motion on the nanometer length scale in real time.

Samples of TNB vapor deposited with $T_{substrate} \approx 0.85T_g$ show a remarkable resistance to translational motion during isothermal annealing at 345 K; no motion was observed on the 12 nm length scale even after 10 000 s. Samples deposited with $T_{substrate} \approx T_g$, in contrast, showed a complete mix-

a)Electronic mail: Ediger@chem.wisc.edu.

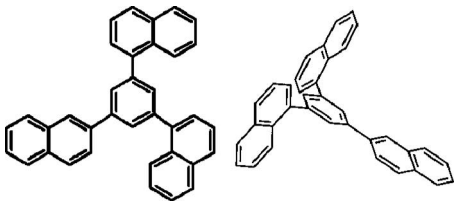

FIG. 1. Structure of 1,3-bis-(1-naphthyl)-5-(2-naphthyl)benzene, or tris-naphthylbenzene (TNB). Left image is a planar view drawn for clarity, while the right image depicts the three dimensional structure of a low energy conformation.

ing on this time and length scale; this result is indicative of the dynamics of a supercooled liquid of TNB. Even faster mixing was observed for samples deposited at $0.56T_g$. These trends with substrate temperature are consistent with the kinetic stability reported for TNB and indomethacin based on differential scanning calorimetry measurements.[5] The NR results for the most stable glasses require that translational motion in these materials is extremely slow, at least 100 times slower than translational motion in the supercooled liquid at the same temperature. The higher density and more efficient packing of the stable glass are responsible for this kinetic stability.

A striking feature of the NR results for the most stable TNB glasses is that the diffraction intensity at all the different diffraction orders decay on the same time scale. This wavevector independent structural reorganization indicates that the extremely long times required for translational motion should not be interpreted as Fickian diffusion with a small diffusion coefficient. Rather we are measuring how long it takes a stable glass to "melt" into the supercooled liquid. For glasses prepared by cooling a supercooled liquid, "melting" back to the liquid is quite rapid once the sample is heated above T_g and generally occurs before the temperature can even be stabilized, obscuring the mechanism of this transformation. In contrast, vapor-deposited stable glasses retain their molecular structure for long periods even above T_g. We argue that the wavevector independent structural reorganization should be interpreted as the growth of liquid regions into the stable glass matrix. One possible mechanism is analogous to the melting of a superheated crystal, where liquid appears first at the surface and then grows into the stable glass from the outside.

EXPERIMENTAL METHODS

The syntheses of 1,3-bis-(1-naphthyl)-5-(2-naphthyl) benzene and 1,3-bis-(1-naphthyl-d_7)-5-(2-naphthyl)benzene have been recently described.[8,9] We will refer to these as protio- and deuterio-TNB, respectively. The molecular structure of TNB is shown in Fig. 1. The molecule is nonplanar, and its intramolecular conformational dynamics have been studied via NMR spectroscopy and molecular mechanics calculations.[9]

Plazek used dilatometry to determine T_g for protio-TNB by cooling the liquid at 1 K/min and reported a value of 342 K.[10,11] This value has been widely used in the literature, and we use it here as a convenient reference temperature for the TNB system; in this paper, we do not use T_g to describe

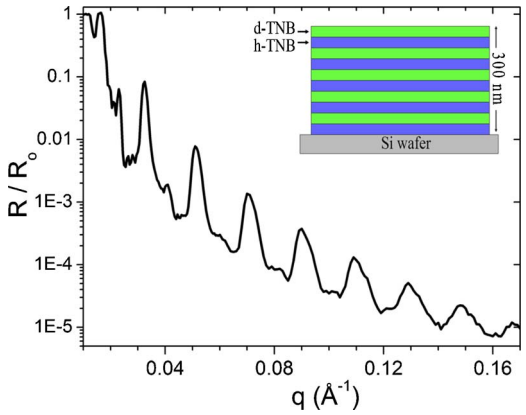

FIG. 2. (Color online) Normalized NR data for a TNB sample vapor deposited at $T_{substrate}=242$ K. Fits (not shown) indicate very sharp interfaces (about 1.5 nm) between protio- and deuterio-TNB. The inset shows the structure of the multilayer films, with five repeating protio/deuterio bilayers. Each layer is ~30 nm. The substrate is a 3 mm thick silicon wafer with native oxide layer.

the state of a particular sample with a particular thermal history. We have performed differential scanning calorimetry measurements on both protio-TNB and deuterio-TNB. After cooling the protio-TNB liquid at 40 K/min to form the glass, we find an onset temperature of 347 K upon heating at 10 K/min. Isotopic substitution influenced the onset temperature by less than 1 K.[3] We assume that protio- and deuterio-TNB form thermodynamically ideal mixtures: these two species are completely miscible and have identical dynamics in these mixtures. Evidence supporting these assumptions has been presented elsewhere.[12]

Thin films of TNB were prepared by physical vapor deposition. Samples were deposited onto 76 mm diameter, 3 mm thick silicon wafers (Wafer World and Virginia Semiconductor). The silicon was used as-received with the native oxide coating. During deposition, the substrate was held at specified temperatures from 192 to 337 K ($0.56T_g$–$0.99T_g$) using a Lakeshore 340 controller with platinum four-wire RTD sensors. The pressure in the vacuum chamber was $\sim 3\times 10^{-8}$ torr before and during the evaporation procedure. Following deposition, the samples were slowly returned to room temperature and held for 1–3 days before being annealed near T_g. The vapor deposited samples contain no detectable impurities as judged by T_g and T_m.[3,5]

For the NR measurements reported here, a repeating bilayer structure of protio- and deuterio-TNB was vapor deposited with 10 total layers and a composite thickness of about 300 nm, as shown in the Fig. 2 (inset). Layer thicknesses were monitored during deposition using a quartz crystal microbalance. Samples were prepared either with a deposition rate of ~1.2 or ~2.5 Å/s. The deposition rate was controlled by the temperature of a quartz crucible containing the crystalline source material. For example, a layer of deuterio-TNB would be deposited by increasing the temperature of the appropriate crucible until the desired deposition rate was established; the crucible temperature was lowered as that layer approached the desired thickness. This procedure conserves TNB but does result in lower deposition rates at the beginning and ending of each layer's deposition. Values for

the total film thickness were determined by ellipsometry, NR, x-ray reflectivity (XR), and the quartz crystal microbalance; the various methods agreed to within 10%.

The NR experiments were conducted at the NIST Center for Neutron Research at the National Institute of Standards and Technology. The NG7 horizontal reflectometer utilized a 4.76 Å collimated neutron beam with a wavelength divergence of 0.18 Å. The angular divergence of the beam was varied through the reflectivity scan and this provided a relative q resolution dq/q of 0.04, where $q=4\pi\sin(\theta)/\lambda$, and θ is the incident and final angle with respect to the surface of the film. Samples were measured during annealing using an in-line oven. The temperature was held constant to within ± 0.1 K during the annealing process, which ranged up to 48 h. The samples and heating oven stabilized at the annealing temperature within 5 min, at which point the first scan was started. Scans were made over a wavevector (q) range from 0.01 $Å^{-1}$ to a maximum of 0.17 $Å^{-1}$, with a typical duration of 30 min/scan. Conversion of the NR spectra, such as shown in Fig. 2, to real-space concentration profiles was done using the REFLFIT program provided by NIST. The thickness of each layer in a given sample was determined by fitting the NR measurements for the first scan obtained during annealing. These thickness values were used in fits of subsequent reflectivity measurements on the same sample.

The total thickness of some of the TNB films was measured before and after annealing using XR at NIST. XR experiments were done on a Bruker AXS diffractometer. A monochromatic x-ray beam ($\lambda=1.54$ Å) was collimated with slits which gave an angular resolution of $\theta=0.000\,14$ radians, such that interference fringes from films as thick as 350 nm could be easily resolved.

RESULTS

Neutron reflectivity

NR was used to measure the concentration profiles of isotopically labeled multilayer thin films (see inset in Fig. 2). The high degree of contrast for neutron scattering between protons and deuterons makes this an ideal technique for monitoring translational motion on molecular length scales. Reflectivity data can be measured *in situ* during annealing to directly follow the evolution of the protio-/deuterio-concentration profile. Detailed information about the NR data and analysis of these multilayer samples has been previously given.[12]

Figure 2 shows the specular NR of a multilayer TNB sample vapor deposited onto a silicon substrate held at 242 K. One can think of the multilayer protio/deuterio structure as a diffraction grating for neutrons.[13–15] Because the interfaces are sharp, many Bragg peaks are evident, extending out to the 17th harmonic. Only odd harmonics are prominent as expected for a sample in which every protio and deuterio layer has the same thickness. To a first approximation, each peak contains information about the amplitude of the Fourier transform of the concentration profile at a particular wavevector q. The fundamental period of the deposited structure is 60 nm, and the peak associated with this is located at the far left of Fig. 2. The peaks at higher q give information on consecutively smaller length scales, corresponding to $d=2\pi/q$. Fits to the data in Fig. 2 indicate an average interfacial breadth of 1.5 nm; this value represents the full width at half height of the derivative of the interfacial concentration profile. Similar values (1–2 nm) are obtained for the roughness of the TNB/air interface by XR. These results suggest that each successive layer filled in depressions in the previous layer but that no further intermixing of the layers occurred during the deposition process. Samples prepared at higher substrate temperatures typically show somewhat broader interfaces, as reported earlier.[3] These broader interfaces indicate that additional isotopic mixing occurred during deposition as a result of surface mobility. As discussed below, stable glass formation occurs as a result of this surface mobility during the deposition process.

These NR experiments only provide information about molecular motion perpendicular to the plane of the film. For high molecular weight polymers in thin films, molecular mobility in the plane of the film may be different than out-of-plane motion[16,17] because spatial confinement leads to anisotropic molecular geometries. Because of its small size and nonpolymeric nature, TNB is not expected to exhibit anisotropic mobility except within a few nanometers of the film surface.

Decay of the structure factor $S(q;t)$

A useful metric for kinetic stability is the time required for a well-defined concentration profile to decay during isothermal annealing. As translational motion blurs the interfaces between protio- and deuterio-TNB layers, the intensity of the Bragg peaks will decrease. This can be measured at each wavevector, giving access to the time-dependent structure factor $S(q;t)$.

Figure 3(a) shows the evolution of the NR for a multilayer sample vapor deposited onto a substrate whose temperature was held near T_g ($T_{\text{substrate}}=330$ K). This sample was annealed at 342 K and NR data were continuously collected, with each scan taking about 30 min. The data have been multiplied by q^4; this removes the Fresnel reflection associated with any flat interface and improves the clarity of presentation. As discussed elsewhere[12] for samples of this structure, the peak height of the third and higher harmonics is approximately related to the square of the amplitude of the Fourier transform of the concentration profile at a particular q:

$$\frac{R_{\text{peak}}-R_{\text{background}}}{(R_{\text{peak}}-R_{\text{background}})_{t=0}} \approx \left[\frac{S(q;t)}{S(q;0)}\right]^2. \tag{1}$$

Here, R_{peak} and $R_{\text{background}}$ indicate the reflectivity values at a peak and the corresponding background reflectivity.

In Fig. 3(a), the decay of the five peaks indicates a gradual blurring of the interfaces between protio- and deuterio-TNB over the roughly 10 h of annealing shown. When a peak decays completely, it indicates that the protio- and deuterio-TNB have become homogeneously mixed on the corresponding length scale. As previously discussed,[12] samples vapor deposited near T_g behave as the equilibrium supercooled liquid during annealing. As shown in Fig. 3(a),

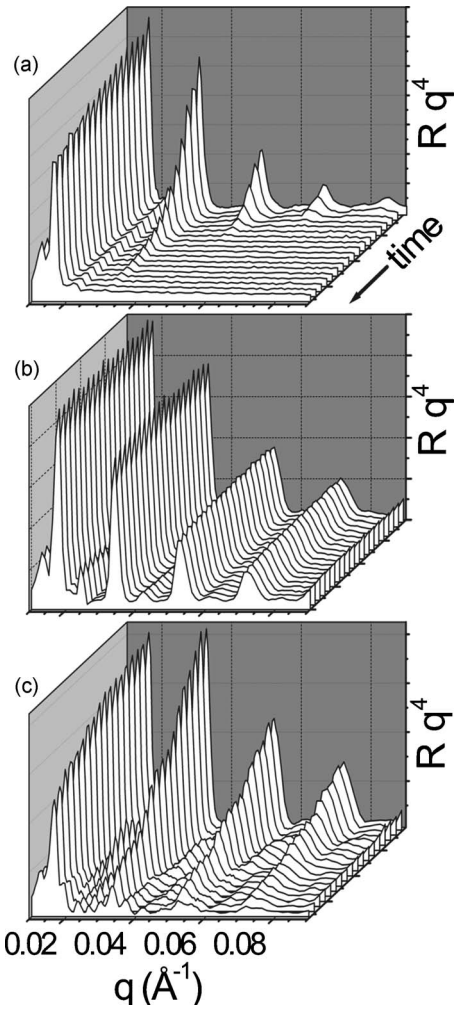

FIG. 3. Time evolution of NR curves during annealing for samples deposited at $T_{substrate}$=330 K (a), 294 K (b), and 242 K (c). Each scan from q =0.01 to 0.09 Å^{-1} required about 30 min, with a total experimental time of about 15 h. Samples (a) and (b) were annealed at 342 K, while (c) was annealed at 345 K. For clarity, the data have been multiplied by q^4 to remove the Fresnel reflection.

the diffraction peaks decay more rapidly as q increases, as expected for Fickian diffusion. The fundamental peak is saturated by multiple scattering events and thus the relationship between its height and $S(q;t)$ is more complicated than indicated in Eq. (1), making it difficult to extract quantitative information about mixing on the 60 nm length scale.

Influence of substrate temperature

Figure 3(b) shows NR curves for a multilayer TNB sample vapor deposited at 294 K ($0.85T_g$). In this case, the annealing temperature was 342 K and the total annealing time shown is about 18 h. Samples deposited at 294 K show a remarkable stability compared to those deposited at higher temperatures [such as Fig. 3(a)]. No relaxation of the concentration profile takes place over the many hours of annealing, indicating that no translational motion is occurring, even on the 10 nm length scale. We emphasize that the only difference in the preparation of the samples shown in Figs. 3(a) and 3(b) is the substrate temperature during vapor deposition.

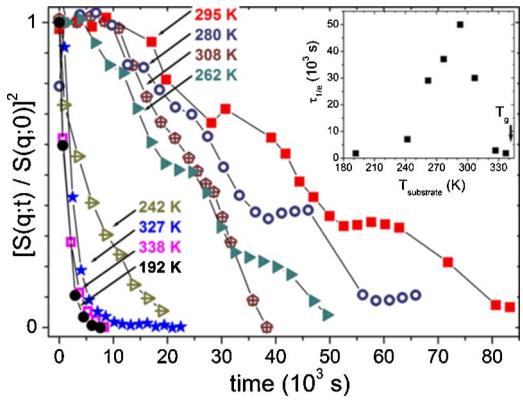

FIG. 4. (Color online) The time-dependent structure factor for multilayer samples annealed at 345 K. Samples were deposited at the indicated temperatures. The structure factor is evaluated for the third harmonic Bragg peak, at $q \approx 0.030$ Å^{-1}. The inset shows the relaxation time $\tau_{1/e}$ plotted as a function of the substrate temperature during vapor deposition.

Figure 3(c) shows the NR curves that result when $T_{substrate}$ is decreased further to 242 K. Here, a substantial decay is observed for all the peaks, although less decay occurs than in Fig. 3(a). Note that decay in Fig. 3(c) is qualitatively different than in Fig. 3(a), with all of the peaks decaying on similar time scales. This feature is clearly inconsistent with Fickian diffusion. The higher annealing temperature used to collect these data (345 K) as compared to other two panels in Fig. 3 (342 K) does not affect these qualitative conclusions.

While the panels in Fig. 3 illustrate the qualitative features of protio-/deuterio-TNB mixing in multilayer samples, quantitative comparisons between samples prepared with different substrate temperatures are more easily made in the format of Fig. 4. Here, we show the decay of the third harmonic ($q \approx 0.03$ Å^{-1}) for vapor-deposited samples annealed at 345 K. We characterize these curves by the time required to decay to $1/e$ of the initial value, $\tau_{1/e}$. A strong dependence of $\tau_{1/e}$ on $T_{substrate}$ is observed. As $T_{substrate}$ is lowered from 337 to 294 K, the 3rd harmonic peak decays more and more slowly, with $\tau_{1/e}$ increasing from 2000 to 50 000 s (see inset). Further lowering of $T_{substrate}$ causes the third harmonic peak to decay more quickly. At the lowest $T_{substrate}$ studied (192 K=$0.56T_g$), the third harmonic decays even faster than for the 337 K deposition.

Figure 4 shows that the functional form of the decay of $S(q;t)$ is qualitatively different for the most stable samples (substrate temperatures between 307 and 262 K). These samples show superexponential decays, with an apparent induction or onset time before any translational motion occurs. These samples also show additional plateaus in the decay of the structure factor, indicating either a spatially heterogeneous process or a highly complex relaxation mechanism. While these plateaus are a common feature in the NR data for stable samples, we would need to perform more depositions and measurements under identical conditions before we can make any quantitative statements about the reproducibility of these features. The stability of glasses formed by vapor deposition sensitively depends on the rate of deposition as

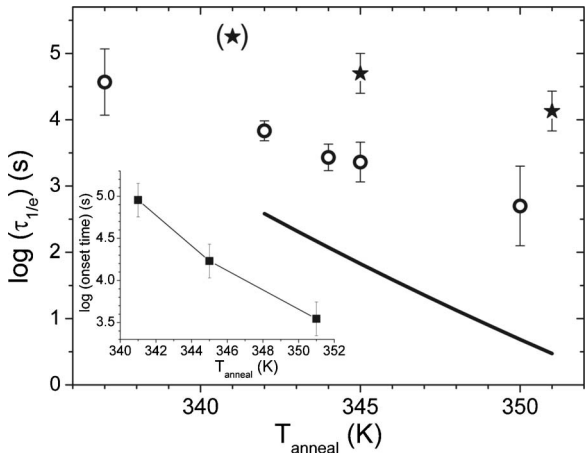

FIG. 5. Structure factor decay time $\tau_{1/e}$ of the third harmonic Bragg peak for an ordinary glass of TNB (deposited at 337 K, open circles) and for a stable glass (deposited at 294 K, stars) as a function of annealing temperature. The thick solid line is a VTF fit to dielectric relaxation measurements of τ_α for supercooled TNB from Richert *et al.* (Ref. 18). The inset shows the log of onset time vs annealing temperature for stable glass samples; the onset time is defined as the time required for $S(q;t)$ to decay to 95% of its initial value. The value of $\tau_{1/e}$ for the stable glass at 341 K is estimated by linear extrapolation of $S(q;t)$ to long times; $S(q;t)$ decayed 40% in 170 000 s.

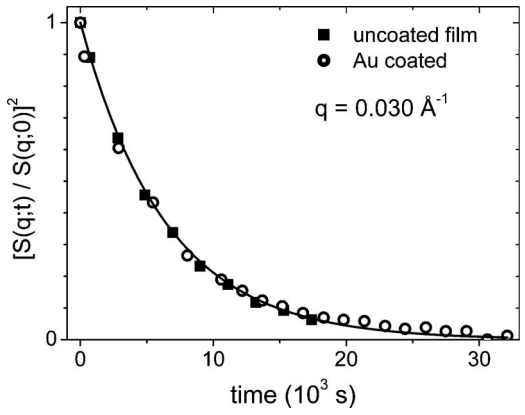

FIG. 6. Time dependent structure factor for the third harmonic for multilayer films deposited at 337 K and annealed at 342 K. Open circles are for a film with a 10 nm gold coating evaporated onto the top surface, while squares are the identical film with no coating. The solid line is a single exponential fit with $\tau_{1/e}$=6700 s.

well as the substrate temperature.[5,6] As discussed below, variations in the deposition rate during the deposition may explain the plateaus seen in Fig. 4.

Annealing temperature dependence

In order to determine the influence of the annealing temperature on the evolution of $S(q;t)$, we performed a series of NR measurements for samples vapor deposited at two temperatures: $T_{substrate}$=294 and 339 K. The samples deposited at 294 K represent our most stable samples, while the samples deposited at 339 K illustrate the behavior of the equilibrium supercooled liquid.

Figure 5 shows $\tau_{1/e}$ for the third harmonic for the stable glass (stars, $T_{substrate}$=294 K) and the supercooled liquid (open circles, $T_{substrate}$=339 K) for annealing temperatures spanning T_g from 337 to 351 K. For comparison, the solid line shows dielectric relaxation measurements of the structural relaxation time τ_α for supercooled protio-TNB, as measured by Richert *et al.*[18] The analysis of the dynamics of the samples deposited at the higher temperature, including calculations of translational diffusion coefficients, has been previously discussed.[12] At all annealing temperatures, the samples deposited at 294 K show substantially slower mixing of the protio- and deuterio-TNB; mixing in stable glasses typically requires annealing about 30 times longer than for the supercooled liquid. For the stable glass, $\tau_{1/e}$ is $300\tau_\alpha$ at 342 K (=T_g) and $3000\tau_\alpha$ at 351 K.

The inset in Fig. 5 shows the onset time, during which these stable glasses could be annealed with no molecular motion apparent at the annealing temperature. The molecules in these glasses are packed so tightly that no translational motion was observed for a full day at 341 K, exceeding τ_α by two orders of magnitude.

The longest annealing times at lower temperatures led to a small degree of crystallization of both stable and ordinary glasses. There was some variability between samples, but the total crystallinity did not exceed 5% of the surface area, as measured by optical microscopy. Previous studies[12] have suggested that this does not influence the observed neutron reflectivity curves and additional tests confirmed this. Two identical samples were prepared at $T_{substrate}$=337 K and, subsequently, one was coated with a 10 nm evaporative gold surface layer. Reflectivity data indicated that the film structure was unperturbed by the gold coating. The gold capping layer completely quenched the crystallization process with no detectable crystallites after 9 h of annealing at 342 K. Figure 6 indicates that the third harmonic $S(q;t)$ decays identically for the two films, showing that neither crystallization nor gold coating has a significant effect on the results reported here. All of the data presented in Figs. 2–5 and 7–9 were acquired on samples without gold coating except for the stable glass sample at the lowest annealing temperature in Fig. 5.

Wavevector dependence of structural evolution

An important feature of NR data like that shown in Fig. 3 is that it simultaneously describes the structural reorganization of our multilayer samples over a range of length scales. Here, we describe the systematic influence of the substrate temperature on the wavevector dependence of the structural reorganization.

Figure 7(a) shows the decay of the third and fifth harmonic Bragg peaks for a sample prepared at $T_{substrate}$ =337 K and annealed at 342 K; the solid lines are exponential fits to the data. The fifth harmonic decays more than twice as fast as the third harmonic, which indicates that homogenization of the sample on the 12 nm length scale occurs more rapidly than on the 20 nm length scale. This behavior is semiquantitatively consistent with Fickian diffusion, as reported earlier,[12] with $S(q;t)/S(q;0) \approx \exp(-q^2Dt)$. The inset shows the concentration profile for a protio-/deuterio-TNB interface obtained by fitting the NR data at several times; the plotted curves are the averaged concentration profile of the

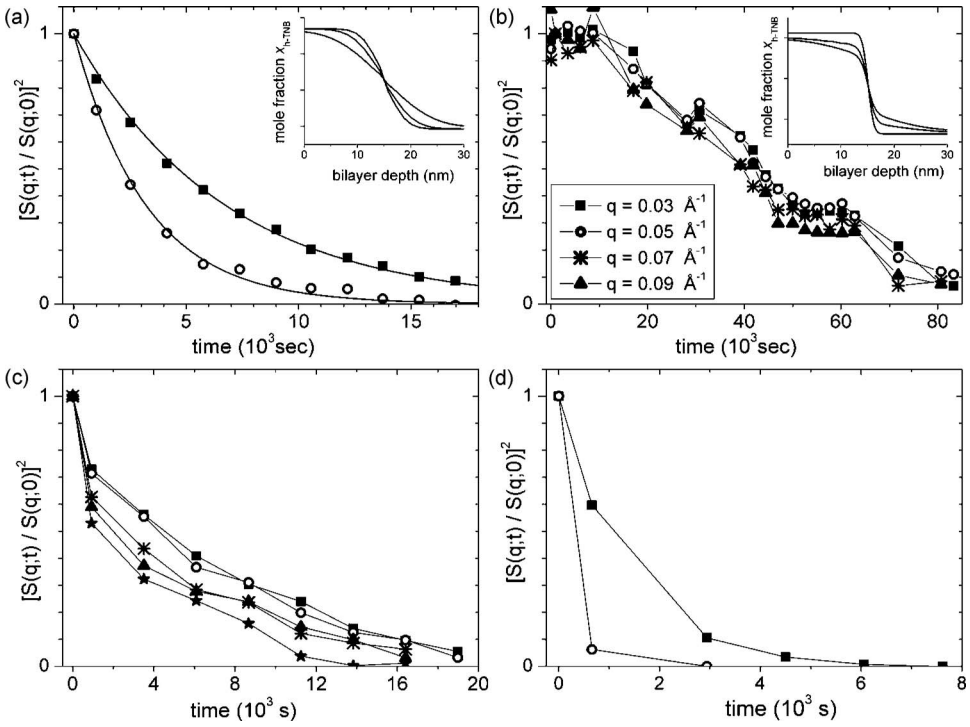

FIG. 7. Time-dependent structure factors for samples deposited at $T_{substrate}$ = 337 K (a), 294 K (b), 242 K (c), and 192 K (d). The data in (a) were obtained during annealing at 342 K; all other data were obtained at 345 K. The solid lines in (a) are single exponential fits to the third and fifth harmonic Bragg peaks, with $\tau_{1/e}$=6700 and 3200 s, respectively. Lines in (b)–(d) are guides to the eye for all harmonics. The inset in (a) is the average concentration profile of the protio/deuterio bilayers within the sample at times t=0, 4100, and 15000 s. The inset in (b) is the average concentration profile at times t=0, 28 000, and 50 000 s.

nine interfaces in the interior of the film. These concentration profiles are qualitatively consistent with the Gaussian broadening expected for Fickian diffusion.

Glasses prepared by deposition onto substrates at 294 K show quite different behaviors, as indicated in Fig. 7(b). All harmonics up to the 13th harmonic decay with the same time dependence; the third through ninth harmonics are shown in Fig. 7(b). Translational motion is highly non-Fickian and is remarkably invariant with length scale. The inset shows the average protio-/deuterio-TNB concentration profile for the nine interior interfaces at various times as obtained by fitting the reflectivity curves. In contrast to the behavior shown in Fig. 7(a), at least some sections of the interface remain quite sharp until $S(q;t)$ has decayed to nearly zero. It is straightforward to illustrate that such concentration profiles must be the proper description of the interface structure. The Fourier transform of a wavevector-independent function, such as the decay function for the harmonics shown, is a delta function in space. The interfacial profile is the integral of this sharp distribution function, which is consistent with the concentration profiles that result from fitting the NR data. For these samples, the reduction in $S(q;t)$ primarily results from a decrease in the size of the sharp concentration step at the interface. The most likely mechanism for the observed structural evolution involves the growth of supercooled liquid regions into the matrix of the stable glass, as we discuss below.

Figures 7(c) and 7(d) plot $S(q;t)$ for samples prepared on substrates at 242 and 192 K, respectively. The sample deposited at 242 K shows behavior that is intermediate between Figs. 7(a) and 7(b); the higher harmonics decay faster

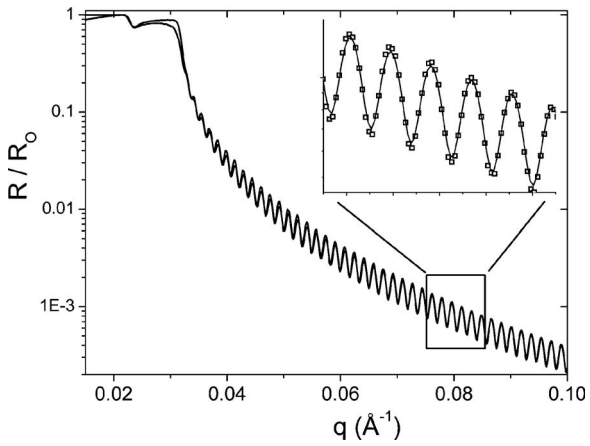

FIG. 8. X-ray reflectivity data (open squares) and fit (solid line) for a sample deposited at 277 K. The total film thickness was 345.4 ± 0.5 nm, with an air/TNB interfacial roughness of 1.0 nm. The inset shows an expanded region for clarity.

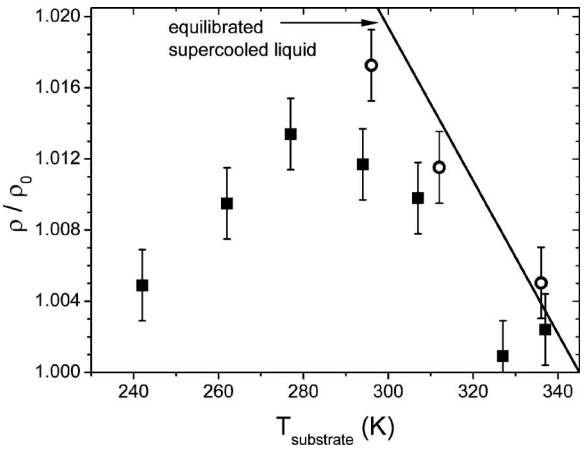

FIG. 9. Densities of as-deposited TNB glasses relative to the density of the ordinary glass as a function of substrate temperature during deposition. Squares indicate deposition at a rate of ~2.5 Å/s, while circles indicate deposition at ~1.2 Å/s. The solid line is a calculation of the expected density if the films had been deposited directly into the supercooled liquid state.

than the lower harmonics but the difference is much smaller than the q^{-2} dependence predicted by Fickian diffusion. Finally, the sample prepared at 192 K shows a much faster decay for the fifth harmonic than for the third harmonic.

The data shown in Figs. 7(b)–7(d) were acquired during annealing at 345 K, while the data shown in Fig. 7(a) were acquired at 342 K. Data for samples like those shown in Fig. 7(a) were also acquired at 345 K, but $S(q;t)$ decays so rapidly that it is difficult to quantitatively analyze the data. The slightly different temperatures used for the experiments shown in Figs. 7(a)–7(d) do not affect the rates at which the various harmonics decay relative to each other.

Density

In conjunction with the reported measurements of translational mobility, we have characterized the thermodynamic properties of our stable glasses. The enthalpy has been obtained from calorimetric experiments.[5] To determine the density of these multilayer TNB samples, we have used XR to measure the thickness of the as-deposited films before and after annealing above T_g.

Figure 8 shows XR data for TNB vapor deposited at 277 K prior to annealing. These data were recorded at room temperature and fitted up to $q=0.21$ Å^{-1}, but only a portion of the data is shown in the figure for clarity. The inset shows an expanded region of the data and fit. The oscillations are Kiessig fringes, which result from interference between x-ray radiation reflected by the air/TNB and TNB/silicon interfaces. Fits to these data also take into account the thin SiO_2 layer on the silicon wafer and roughness of the interfaces. For this sample, the fit gives a total film thickness of 345.4 ± 0.5 nm. After annealing this sample at 345 K for 1 day, NR data showed that the concentration profile was fully relaxed and we assume that the film had reached the equilibrium supercooled liquid state. The sample was cooled back to room temperature and a second XR curve was acquired. The inverse of the ratio of these thicknesses is equal to the ratio of the densities for the as-deposited and ordinary glass.

Figure 9 shows the measured density ratio of the as-deposited glass and the ordinary glass for substrate temperatures between 342 and 242 K, with all of the thickness measurements performed at room temperature. The samples shown as squares were vapor deposited at about 2.5 Å/s, while the open circles indicate a rate of about 1.2 Å/s. Both series of samples show that the densities of vapor-deposited glasses increase with decreasing substrate temperature down to 294 K. At even lower deposition temperatures, the trend is reversed. Note that the substrate temperature that maximizes the density also results in the slowest translational motion (Fig. 4). While the two sets of samples in Fig. 9 agree qualitatively, higher densities were measured for glasses deposited at lower deposition rates. It has recently been shown that, in this temperature regime, lower deposition rates lead to glasses with lower enthalpy and higher kinetic stability;[6] it is reasonable that these properties would be associated with more dense molecular packing.

All of the TNB samples prepared by vapor deposition had measured densities at least as large as the corresponding ordinary glass. Since all of the XR measurements were performed at room temperature, we cannot exclude the possibility that density changes occurred in the as-deposited films prior to measurement. For the lowest temperature point at 242 K, it is possible that the as-deposited glass was lower in density than the ordinary glass but that densification occurred during the 2 days that this sample was held at room temperature before measurement.

The solid line in Fig. 9 is the density expected for a supercooled liquid in equilibrium at the deposition temperature. It is based on an extrapolation of the density data for the supercooled liquid with a correction for the geometry of these experiments. A thin glassy film in contact with a rigid substrate undergoes deformation during temperature changes if the substrate has a different thermal expansion coefficient than the glass. For these experiments, the thermal expansion coefficient of the silicon wafer is negligible and a TNB glass is placed in tension during cooling. As described by Bauer *et al.*,[19] the thickness of a glass film under these conditions depends on Poisson's ratio ν. Changes in the thickness with temperature are calculated by using the following relationship: $\alpha_{obs}=\alpha_p(1+\nu)/(1-\nu)$, where α_{obs} is the observed linear thermal expansion coefficient normal to the substrate and α_p is the usual constant pressure linear expansion coefficient. For this calculation, we assume $\nu=0.33$ in the glass. In calculating the line shown in Fig. 9, we assume that the supercooled liquid leaves equilibrium at 345 K upon cooling; this is reasonable given that most of these samples were cooled relatively quickly from this temperature.

The close agreement between the solid line in Fig. 8 and the density ratios for the more slowly deposited samples (circles) indicates that these materials were prepared with densities close to that of the equilibrium supercooled liquid.

DISCUSSION

Mechanism of stable glass formation

We have shown elsewhere[3,5,6] that stable glasses can be prepared with vapor deposition because dynamics at the glass surface can be many orders of magnitude faster than dynamics in the bulk.[20–22] Molecules within a few nanometers of the surface have time to find low energy packing configurations before they are buried by further deposition. All of the data presented here support this mechanism. Both the kinetic stability (Fig. 4) and the density (Fig. 9) of TNB glasses are maximized when the substrate temperature is $0.85T_g$. Similar behavior has been observed in differential scanning colorimetry (DSC) measurements on vapor-deposited indomethacin. In this case, the onset temperature for mobility was maximized for a substrate temperature of $0.85T_g$. When substrates are held at higher temperatures very near T_g, surface equilibration should be very rapid and nearly complete. We expect to form glasses in this regime whose properties are essentially those of an equilibrium supercooled liquid at the substrate temperature; these materials are as stable as they can be (without crystallizing). As the substrate temperature is lowered, surface mobility slows to the point that equilibration during vapor deposition is far from

completion. At the lowest substrate temperatures, the substrate is so cold that the surface is no longer mobile. Molecules then hit the surface and stick without any rearrangement creating low density, low stability films. Deposition between these two extremes maximizes the effects of the enhanced surface mobility and thus creates the most stable glasses.

Although we have not varied the deposition rate across a wide range in this study, over a limited range we find results that support the surface mobility mechanism. Lower deposition rates provide more time for surface equilibration[6] and thus lead to glasses with higher density, as shown in Fig. 9.

Although surface heating is not the focus of this current study, it is instructive to rule out the possibility of surface heating during vapor deposition as a mechanism for the enhanced mobility, leading to stable glasses. The total thermal energy incident on the film can be calculated from the adsorbing vapor phase molecules and from radiative heating due to the vaporization crucible. For the thin films studied here, the resulting thermal gradients normal to the film would be at most a few millikelvins. Additionally, the DSC data presented elsewhere indicate that lower crucible temperatures lead to more stable glasses.[6] This result contradicts the hypothesis that stability results from a temperature gradient in the film.

Isothermal kinetic stability of stable glasses

Some of the vapor-deposited TNB glasses show a remarkable isothermal stability and here we make a comparison with the aging experiments of Kovacs on polyvinylacetate.[4] The most stable sample that Kovacs prepared was annealed for nearly 2 months at 298 K ($\sim T_g - 10$ K). Upon heating to 313 K, the volume of this sample recovered to its equilibrium volume in a time that is equal to 30 times the structural relaxation time τ_α at 313 K (as estimated from the volume response after minimal annealing at 298 K). This ratio of the equilibration time to τ_α is a reasonable figure of merit for isothermal kinetic stability. Figure 7(b) shows a TNB sample in which no detectable molecular motion occurred for 10 000 s during annealing at 345 K. At this temperature, τ_α is 80 s as measured by dielectric relaxation. Thus, this TNB sample showed no indication of even beginning relaxation toward equilibrium for a time exceeding $100\tau_\alpha$. This rather conservative comparison indicates that vapor-deposited TNB samples have greater kinetic stability than traditional glasses that have been annealed below T_g for very long times.

Mechanism of the glass-to-liquid transformation

In this section, we discuss the mechanism by which an extremely stable glass is transformed into a supercooled liquid upon heating above T_g. For the experiments reported here, the stable glass has a density which exceeds that of the supercooled liquid by $\sim 1.5\%$ (Fig. 9). Furthermore, the stable glass is about 10 J/g lower on the potential energy landscape than the supercooled liquid.[6] Thus, in comparison to the supercooled liquid, the molecules in the stable glass are tightly packed into low energy configurations. It is difficult for them to escape this packing and find configuration characteristics of the supercooled liquid. Qualitatively, this explains the observation that the stable glass can persist more than $100\tau_\alpha$ without any indication of transformation to the supercooled liquid. This separation of time scales provides a new opportunity to study the glass-to-liquid transformation. When an ordinary glass is heated to T_g, the transformation process occurs on the same time scale as liquid relaxation, obscuring the distinction between these processes. In contrast, stable glasses allow the transformation process to be studied without this interference.

We draw inspiration for describing the stable glass-to-liquid transformation from experiments where a system at thermodynamic equilibrium is "jumped" into a different region of the phase diagram. For example, when the temperature or pressure of a polymer blend in the one phase region is suddenly jumped into the two phase region, the system responds in one of two ways. Either the blend immediately begins to phase separate everywhere in the sample (spinodal decomposition) or phase separation proceeds by nucleation and growth.[23,24] In this latter case, small regions, whose compositions are at or near the new equilibrium composition, grow into the homogeneous liquid. Nucleation sites can either be distributed throughout the sample or nucleation can preferentially occur at surfaces and interfaces. For a one component system, a somewhat analogous situation is the superheating of a crystal. The liquid phase appears first at the surface of the crystal and then grows toward the interior until the phase transformation is complete.[25] Experiments and simulations indicate that crystals can be superheated considerably above their melting points if surface nucleation can be prevented.[26,27] In loose analogy to a superheated crystal, our stable glasses have been "superheated" when the temperature is increased above T_g; eventually, the glasses melt into the supercooled liquid. The stable glass-to-liquid transformation is not completely analogous to the examples above since the stable glass is not a metastable state. Nevertheless, we assume that spinodal decomposition or a process with a growth front are the only plausible mechanisms for the transformation of the stable glass into the supercooled liquid.

The decay of $S(q;t)$ for various harmonics of our multilayer stable glass samples, as shown in Fig. 7(b), indicates that the stable glass-to-liquid transformation likely occurs by growth of the liquid into the stable glass. All Bragg peaks, for the 3rd–13th harmonics, require longer than 80 000 s to decay to zero [only the third to ninth are shown in Fig. 7(b) for clarity]. Thus, molecules in some portions of the sample have moved less than the 5 nm length scale probed by the 13th harmonic ($q=0.13$ Å^{-1}) during the full annealing time. These portions of the sample cannot be in the liquid state. Figure 7(a) shows that even the fifth harmonic of the supercooled liquid has decayed to zero at times much earlier than 80 000 s. This feature of the data tells us that translational motion in the stable glass is very slow and gives an upper bound on the diffusion coefficient $[D \approx (q^2\tau)^{-1}]$ in the stable glass of $\sim 10^{-19}$ cm^2/s at 345 K. This is an upper bound because it is possible that no motion occurs in the stable glass on the 80 000 s time scale and that all the decay of $S(q;t)$ can be attributed to the melting of the glass into the

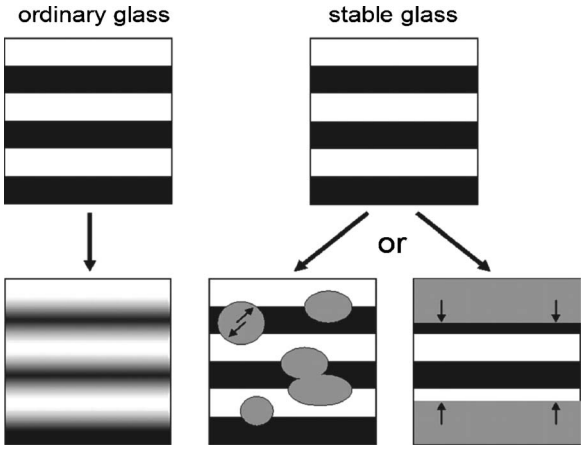

FIG. 10. Schematic view of structural evolution for a multilayer film of an ordinary glass and a stable glass. The ordinary glass evolves by Fickian diffusion, with Gaussian broadening of the interfaces due to translational diffusion. In contrast, the stable glass evolves by the growth of liquid regions (growth indicated by small arrows). The center pathway shows the growth of liquid bubbles from the interior of the film. The right pathway shows liquid growth beginning at the free surface and the interface with silicon with subsequent growth of the liquid phase toward the center of the film. Consistent with the NR results, both stable glass scenarios maintain some sharp protio/deuterio interfaces even at long times.

liquid. For comparison, based on Figs. 5 and 7(a), we estimate D for the supercooled liquid at 345 K to be about 500 times larger than this estimate for the stable glass, which is consistent with an earlier study[12] in this q range.

The simultaneous decay of $S(q;t)$ for all wavevectors in the range corresponding to the 3rd–13th harmonics of our multilayer structures allows us to estimate the size of the liquid regions that are growing into the stable glass. The third harmonic decay describes mixing on the 20 nm length scale, and thus, at the point where an appreciable fraction of the stable glass has transformed into the liquid, the liquid regions are 20 nm or larger.

Figure 10 schematically illustrates our explanations for the decay of $S(q;t)$ that occurs when an ordinary glass and a stable glass are annealed above T_g. The left side of the figure illustrates Fickian diffusion; we use this as an approximate model for translational motion in the supercooled liquid that forms immediately upon heating the ordinary glass. As discussed above, Fickian diffusion gives rise to a wavevector dependent decay with $S(q;t) \propto q^{-2}$. The right side of Fig. 10 presents two possible liquid growth models for the transformation of the stable glass into the supercooled liquid. The far right pathway shows liquid regions at the top and bottom of a thin film growing into the interior of the stable glass. The center pathway represents "bubbles" of the supercooled liquid growing into the stable glass. Both stable glass scenarios show that sharp protio/deuterio interfaces remain in the sample even after a substantial portion of the stable glass has transformed into the liquid, which is in agreement with the concentration profiles shown in the inset of Fig. 7(b). It is the persistence of this sharp interface that explains the wavevector independence of the decay of $S(q;t)$ as discussed above. As a consistency check, we note that translational motion in the supercooled liquid is sufficiently fast to thoroughly mix protio- and deuterio-TNB on the 20 nm length scale on the time scale of 10^4 s. Thus, we portray the liquid regions in the stable glass scenarios of Fig. 10 at a uniform contrast level intermediate between the protio- and deuterio-TNB.

Of the two growth scenarios shown on the right side of Fig. 10, we tentatively favor liquid growth from the top (free surface) and bottom (substrate) interfaces. When we freely fit the NR curves from Fig. 7(b), the concentration profiles at intermediate times show substantial mixing at the top and bottom of the multilayer films with unperturbed concentration profiles in the center of the film. It is also possible to fit the reflectivity data to a simple bubble growth model but this fit is not as good. The surface growth mechanism can also provide a tentative interpretation of the multiple plateaus seen in the decays of $S(q;t)$ for the most stable glasses (Fig. 4). As described in the Experimental section, the deposition rate was modulated as the multilayer samples were prepared; a series of layers of more stable glass would be expected to result and these could temporarily slow the growth of liquid toward the interior of the film.

The glass-to-liquid transformation mechanism may be analogous to the surface directed spinodal decomposition seen in thin films of some isotopic polymer mixtures.[28] During annealing, phase separation is directed by the free surface such that structure propagates into the film several hundred nanometers. In these cases, surface initiation of an oriented structure is due to the lower energy of the deuterated species at the free surface.

We do not claim that the data presented here unambiguously establish that the growth of liquid regions is the correct mechanism for the transformation of the stable glass into the supercooled liquid. However, the wavevector independence of the decay of $S(q;t)$ demands that sharp protio/deuterio interfaces remain in the sample until the very last stages of the transformation. The growth of liquid regions into the stable glass seems to be the most reasonable interpretation of this feature. The only alternative of which we are aware would be extremely non-Fickian diffusion.[29,30] Models of this type have been developed to describe diffusion in equilibrium supercooled liquids and take into account spatial heterogeneity in dynamics. Simulations provide evidence that on sufficiently small length scales such models are realistic for equilibrium supercooled liquids.[31] The current NR data is broadly consistent with this view or with either of the models shown on the right of Fig. 10. Further experiments should distinguish between these possibilities.

A "growth" mechanism for transforming a stable glass into the supercooled liquid would be broadly consistent with a number of different scenarios. Kurita and Tanaka[32] and Matyushov and Angell[33] have argued that fragile liquids undergo a first-order liquid/liquid transition near T_g. If the stable glasses of TNB are associated with a different liquid than the easily accessible supercooled liquid, then the transformation observed here would be similar to the nucleation and growth reported by Tanaka in triphenylphosphite. Garrahan *et al.*[34] have argued that kinetically constrained models of glass formers have dynamics at a first-order coexistence line between active and inactive phases. The stable glasses of TNB may be similar to the inactive phase in this picture and the active phase could appear by growth from the surface.

More generally, the kinetics we report could be considered to be exaggerated versions of the autocatalytic volume recovery[35] observed when moderately stable polymer glasses are heated above T_g.

CONCLUSIONS

The very slow transformation kinetics of stable glasses produced by vapor deposition, relative to the structural relaxation time of the liquid, provides a new opportunity to understand the mechanism of the glass-to-liquid transformation. By preparing isotopically labeled multilayer samples of tris(naphthylbenzene), we can directly observe translational motion near T_g on the 5–20 nm length scale. Deposition within a few kelvins of T_g produces the ordinary supercooled liquid; subsequent annealing generates the broad interfaces characteristic of Fickian diffusion. In contrast, deposition onto a substrate at $0.85T_g$ produces highly stable glasses. Some sharp interfaces remain in these samples even after annealing has transformed most of the stable glass into the supercooled liquid. The experimental results are consistent either with the growth of the supercooled liquid into the stable glass from the film surfaces or with bubble growth in the interior of the film. Similar mechanisms may be relevant whenever an even moderately stable glass is heated above T_g.

ACKNOWLEDGMENTS

We gratefully acknowledge the support of NSF Chemistry (No. 0605136). We thank Austen Angell, Nitash Balsara, Peter Harrowell, and John Perepezko for useful discussions. Any mention of commercial products in this paper does not imply recommendation or endorsement by NIST.

[1] M. Dussauze, A. Giannoudakos, L. Velli, C. P. E. Varsamis, M. Kompitsas, and E. I. Kamitsos, J. Chem. Phys. **127**, 034704 (2007).
[2] S. L. Simon, J. W. Sobieski, and D. J. Plazek, Polymer **42**, 2555 (2001).
[3] S. F. Swallen, K. L. Kearns, M. K. Mapes, Y. S. Kim, R. J. McMahon, M. D. Ediger, T. Wu, L. Yu, and S. Satija, Science **315**, 353 (2007).
[4] A. J. Kovacs, Fortschr. Hochpolym.-Forsch. **3**, 394 (1963).
[5] K. L. Kearns, S. F. Swallen, M. D. Ediger, T. Wu, and L. Yu, J. Chem. Phys. **127**, 154702 (2007).
[6] K. L. Kearns, S. F. Swallen, M. D. Ediger, T. Wu, Y. Sun, and L. Yu, J. Phys. Chem. B **112**, 4934 (2007).
[7] K. Ishii, H. Nakayama, S. Hirabayashi, and R. Moriyama, "Anomalously high-density ethylbenzene glass prepared by vapor deposition at temperatures close to the glass-transition temperature," Chem. Phys. Lett., accepted (2008).
[8] P. A. Bonvallet, C. J. Breitkreuz, Y. S. Kim, E. M. Todd, K. Traynor, C. G. Fry, M. D. Ediger, and R. J. McMahon, J. Org. Chem. **72**, 10051 (2007).
[9] C. M. Whitaker and R. J. McMahon, J. Phys. Chem. **100**, 1081 (1996).
[10] D. J. Plazek and J. H. Magill, J. Chem. Phys. **49**, 3678 (1968).
[11] D. J. Plazek and J. H. Magill, J. Chem. Phys. **45**, 3038 (1966).
[12] S. F. Swallen, M. K. Mapes, Y. S. Kim, R. J. McMahon, M. D. Ediger, and S. Satija, J. Chem. Phys. **124**, 184501 (2006).
[13] S. M. Baker, G. S. Smith, N. J. S. Brown, M. Nastasi, and K. Hubbard, Phys. Rev. B **55**, 7255 (1997).
[14] M. Gupta, A. Gupta, J. Stahn, M. Horisberger, T. Gutberlet, and P. Allenspach, Phys. Rev. B **70**, 184206 (2004).
[15] E. Sivaniah, R. A. L. Jones, and M. Sferrazza, Phys. Rev. E **67**, 052801 (2003).
[16] S. Narayanan, D. R. Lee, R. S. Guico, S. K. Sinha, and J. Wang, Phys. Rev. Lett. **94**, 145504 (2005).
[17] K. Tawa and K. Wolfgang, Macromolecules **35**, 7018 (2002).
[18] R. Richert, K. Duvvuri, and L.-T. Duong, J. Chem. Phys. **118**, 1828 (2003).
[19] C. Bauer, R. Bohmer, S. Moreno-Flores, R. Richert, H. Sillescu, and D. Neher, Phys. Rev. E **61**, 1755 (2000).
[20] R. C. Bell, H. F. Wang, M. J. Iedema, and J. P. Cowin, J. Am. Chem. Soc. **125**, 5176 (2003).
[21] C. J. Ellison and J. M. Torkelson, Nat. Mater. **2**, 695 (2003).
[22] J. S. Sharp and J. A. Forrest, Phys. Rev. Lett. **91**, 235701 (2003).
[23] N. P. Balsara, C. Lin, and B. Hammouda, Phys. Rev. Lett. **77**, 3847 (1996).
[24] J. W. Gibbs, *The Scientific Papers of J. Willard Gibbs* (Dover, New York, 1961).
[25] T. Nguyen, P. S. Ho, T. Kwok, C. Nitta, and S. Yip, Phys. Rev. B **46**, 6050 (1992).
[26] J. Daeges, H. Gleiter, and J. H. Perepezko, Phys. Lett. A **119**, 79 (1986).
[27] M. Forsblom and G. Grimvall, Nat. Mater. **4**, 388 (2005).
[28] R. A. L. Jones, L. J. Norton, E. J. Kramer, F. S. Bates, and P. Wiltzius, Phys. Rev. Lett. **66**, 1326 (1991).
[29] L. Berthier, D. Chandler, and J. P. Garrahan, Europhys. Lett. **69**, 320 (2005).
[30] K. S. Schweizer and E. J. Saltzman, J. Phys. Chem. B **108**, 19729 (2004).
[31] L. Berthier, Phys. Rev. E **69**, 020201 (2004).
[32] R. Kurita and H. Tanaka, Science **306**, 845 (2004).
[33] D. V. Matyushov and C. A. Angell, J. Chem. Phys. **126**, 094501 (2007).
[34] J. P. Garrahan, R. L. Jack, V. Lecomte, E. Pitard, K. van Duijvendijk, and F. van Wijland, Phys. Rev. Lett. **98**, 195702 (2007).
[35] G. B. McKenna, in *Comprehensive Polymer Science*, edited by C. Booth and C. Price (Pergamon, Oxford, 1991), Vol. 2, p. 311.